Journal of Catalysis 286 (2012) 206–213

Contents lists available at SciVerse ScienceDirect

Journal of Catalysis

journal homepage: www.elsevier.com/locate/jcat

Rubidium- and caesium-doped silicotungstic acid catalysts supported on alumina for the catalytic dehydration of glycerol to acrolein

Muhammad H. Haider [a], Nicholas F. Dummer [a], Dazhi Zhang [b], Peter Miedziak [a], Thomas E. Davies [a], Stuart H. Taylor [a], David J. Willock [a], David W. Knight [a], David Chadwick [b], Graham J. Hutchings [a,*]

[a] Cardiff Catalysis Institute, School of Chemistry, Cardiff University, Cardiff CF10 3AT, UK
[b] Department of Chemical Engineering, Imperial College London, South Kensington Campus, London SW7 2AZ, UK

ARTICLE INFO

Article history:
Received 17 July 2011
Revised 18 October 2011
Accepted 6 November 2011
Available online 15 December 2011

Keywords:
Glycerol dehydration
Acrolein
Silicotungstic acid
Caesium-doped catalysts
Supported heteropoly acids

ABSTRACT

Dehydration of glycerol was carried out using rubidium- and caesium-doped silicotungstic acid catalysts. These catalysts were prepared by varying concentration of the dopant metal cations while keeping the concentration of heteropoly acid unchanged. High acrolein selectivity (94–96%) was observed with unsupported caesium-doped silicotungstic acid and rubidium-doped silicotungstic acid with a dilute glycerol feed (0.5 wt.% in water). These catalysts were then supported on alpha-alumina and an alumina comprising a theta-delta mixture. Caesium-doped silicotungstic acid supported on theta-delta alumina gave a maximum selectivity of *ca.* 90% at 100% glycerol conversion for 90-h time online, with a 10 wt.% glycerol solution. With a more concentrated glycerol feed (20 wt.%), this catalyst achieved a space time yield of 210 $g_{(acrolein)}$ $kg^{-1}_{(cat)}$ h^{-1}. The catalyst was investigated further to determine the origin of the long-term stability. The binding strength of the partially doped silicotungstic acid on the alumina was found to be crucial to sustain the supported Keggin structure and hence the acidity of the active sites resulting in a high acrolein yield.

1. Introduction

The conversion of biomass and biomass-derived feed stocks into valuable chemicals and fuels is emerging as an important aspect of modern chemical processes [1]. Presently, transesterification of plant oils is increasing as this process yields biodiesel and also glycerol as a by-product [2,3]. Increasingly, utilisation of glycerol as a versatile starting a material is concurrent with both its increasing availability and chemical properties. The structure of glycerol contains three hydroxyl groups, which makes it readily soluble in water and other alcohols, and it can undergo chemical and biochemical changes because of its ability to be functionalised [4]. The efficient chemical transformation of glycerol to acrolein forms an appreciable contribution to current efforts to obtain value-added products derived from biomass.

Acrolein is an important chemical intermediate in the manufacture of polymers, and it is presently produced industrially in the order of several million tonnes per annum from propene [5–7]. However, its preparation from glycerol is advantageous as this pathway can be viewed as being based on a renewable feedstock [3,8]. When glycerol is subjected to acidic conditions, it quickly undergoes decomposition with the release of water and other products. Typically, in order to dehydrate glycerol, high temperatures along with acidic conditions are required. Acidity plays a vital role in glycerol dehydration controlling the selectivity to acrolein, and acidic catalysts having a Hammett acidity (HA) [9] below 2 are considered desirable in this regard [10]. Tungstated zirconia catalysts have been evaluated for glycerol conversion to acrolein at a temperature of 300 °C, and they were found to be active [11]. Tungsten was found to increase the acidity of the catalyst; however, the stability of such catalysts at extended reaction times remains a problem. This may be due to the high acidity of the catalysts, which is thought to be responsible for coke formation and ultimately lack of stability observed [12]. The effect of acidity on the stability of catalysts for the dehydration of glycerol has been studied by grafting zirconia onto silica [12]. Comparison of the grafted and ungrafted catalysts appeared to differ with respect to stability, with the zirconia-grafted catalyst being more stable. This effect was attributed to a minor distortion in the structure of the heteropoly acid (HPA), and its binding strength to the support, leading to a decrease in acidity and in turn an increase in the stability of the catalysts [4]. Chai and co-workers [13,14] conducted studies of glycerol dehydration using different niobium oxide-based catalysts, which resulted in an acrolein selectivity of 50% at a glycerol conversion of 90%. Use of basic materials, *e.g.* MgO, did not result in acrolein formation, whereas it was observed with slightly acidic, *e.g.* ZrO_2, and highly acidic, *e.g.* H_3PO_4/Al_2O_3,

* Corresponding author.
E-mail address: hutch@cardiff.ac.uk (G.J. Hutchings).

0021-9517/$ - see front matter © 2011 Elsevier Inc. All rights reserved.
doi:10.1016/j.jcat.2011.11.004

catalysts. Notably, acrolein selectivity increased with increasing acidity from slightly acidic (30%) with Hammet acidity between −3 and +7 to highly acidic catalysts (70%) with Hammet acidity between −8 and −3, showing that acidity was definitely exerting a role in controlling the acrolein selectivity.

Supported heteropoly acid catalysts are very acidic, typically with a Hammet acidity of *ca.* −9, and they have been used in the catalytic dehydration of glycerol [15]. Different loadings of silicotungstic acid (STA), supported on silica or carbon, have been investigated; however, these catalysts were also found to be unstable [16]. Zirconia-supported HPA catalysts were found to be more thermally stable, with an improved dispersion of the HPA active phase, and this was found to be a key factor in tuning the activity and selectivity towards acrolein [15,17]. HPAs supported on Al_2O_3 have been studied [4] notably by Martin et al. [18]. While high acrolein selectivities (70–80%) could be obtained, rapid deactivation was observed. This was thought to be due to structural changes in the HPA active phase at high temperatures or the blocking of the acid sites on the HPA due to coking. Phosphotungstic acid (PTA) and phosphomolybidic acid (PMA) HPAs were also evaluated for glycerol dehydration [18,19], and high selectivities were observed. These catalysts were very active and selective towards acrolein achieving a selectivity of up to 98% at 100% glycerol conversion but were found to have short lifetimes due to coking [20]. Addition of alkaline and alkaline earth cations to these catalysts improved the performance, but they were still found to deactivate over a short reaction time [21].

It is therefore clear that for the application of this class of catalyst to be viable on a larger scale, catalyst deactivation must be overcome. One strategy to reduce deactivation has been to co-feed oxygen in an effort to reduce the accumulation of coke on the catalyst [22]. One approach adopted by Dubois and co-workers involved the pre-treatment of the titania support with Cs^+ followed by impregnation by the phosphotungstic acid with co-fed oxygen in the reaction stream [23]. These catalysts maintained glycerol conversion of *ca.* 98% for 21 h with 78% acrolein yield [23]. However, the inclusion of oxygen increased the concentration of CO_2 and other oxygenated products and consequently decreased the acrolein selectivity.

Against this background, we have developed caesium and rubidium exchanged silicotungstic acids as catalysts for glycerol dehydration to acrolein, and we have also investigated the effect of supporting them on two different types of alumina. A major aim of the work was to determine whether stable catalysts could be prepared and operated in the absence of co-fed oxygen for the transformation of relatively high concentrations of glycerol in an aqueous feed.

2. Experimental

2.1. Materials

Glycerol (99% *Sigma Aldrich*) was used as received. For the catalyst preparation, silicotungstic acid $\{H_4[SiW_{12}O_{40}]\text{-}nH_2O$,HSiW} (HSiW, 99.9% *Sigma Aldrich*) and rubidium acetate and caesium carbonate (*Sigma Aldrich*) were used. Two types of alumina supports were used: α-Al_2O_3 (Al_2O_3-1) and a mixture of delta and theta Al_2O_3 (Al_2O_3-2) both supplied by Vertellus Speciality Chemicals.

2.2. Catalyst preparation

2.2.1. Silicotungstic acid on alumina catalysts

A series of catalysts with different wt.% loadings of silicotungstic acid (STA) (10%, 20%, 30%, 40% and 50%) on Al_2O_3-1 were prepared by means of an incipient wetness method. The method included the mixing of aqueous solution (5 mL H_2O per g of catalyst) of heteropoly acid with the support and stirring it for 20 h followed by drying (110 °C, 16 h). The same method was followed to prepare 30% silicotungstic acid supported on theta-delta Al_2O_3-2. These catalysts are referred to as follows: untreated Al_2O_3-1 as 0STA-1, 20STA-1, 30STA-1, 40STA-1, 50STA-1 and 30STA-2.

2.2.2. Caesium- and rubidium-doped silicotungstic acid (STA) catalysts

Different caesium-doped STA catalysts were prepared using aqueous solutions of caesium carbonate (0.05, 0.15, 0.25 and 0.35 mol) in deionised water (10 mL), respectively. Separately, an aqueous solution of STA (0.06 M/20 mL) was prepared. The caesium solution was added dropwise to the STA solution with stirring over 30 min and then dried (110 °C, 16 h). Similarly, rubidium-doped STA catalysts were prepared with rubidium acetate. These catalysts are referred to as caesium (0.05 M)-doped silicotungstic acid (0.06 M): Cs0.05/STA, Cs0.15/STA, Cs0.25/STA, Cs0.35/STA, Rb0.05/STA, Rb0.15/STA and Rb0.25/STA.

2.2.3. Cs-doped HPAs (silicotungstic acid, silicomolybidic acid and phosphomolybidic acid) Catalysts

Further caesium (0.25 M)-doped HPAs were also prepared from an aqueous solution of caesium carbonate (0.25 M/10 mL) and aqueous solutions (0.06 M/20 mL) of HPAs (silicotungstic acid, silicomolybidic acid: SMA and phosphomolybidic acid: PMA). A caesium solution was added dropwise to the aqueous solution of HPAs, respectively, while stirring. This process turned the clear solution of HPAs opaque, indicating precipitation of the catalyst. Stirring was continued for 30 min followed by drying at 110 °C overnight. These catalysts are denoted as Cs/STA, Cs/SMA and Cs/PMA.

2.2.4. Cs- and Rb-doped STA supported on Al_2O_3-1 and Al_2O_3-2 catalysts

0.05 M solutions of caesium and rubidium salts were prepared from their carbonate and acetates, respectively, in 10 mL of deionised water. Metal solutions were added dropwise into the STA (0.06 M) solution, respectively, followed by the addition of the Al_2O_3-1 support while stirring. Stirring was continued for 20 h followed by drying at 110 °C for 16 h. The same procedure was followed for preparing Al_2O_3-2-supported catalysts. These catalysts are referred to as caesium-doped silicotungstic acid supported on Al_2O_3; Cs/STA-1, Rb/STA-1, Cs/STA-2 and Rb/STA-2.

2.3. Catalyst characterisation

BET surface area analysis was carried out by means of nitrogen adsorption using a Micromeritics Gemini instrument. Prior to analysis, all the samples were degassed (120 °C, 1 h) using a Micromeritics Flow prep 060 instrument. Powder XRD analysis was conducted with an XpertPro Panalytical instrument using a Cu radiation source producing Kα monochromatic X-rays. The pattern was collected over the 2θ range of 10–80°. Raman spectroscopy was carried out with a Renishaw inVia Raman Microscope using a 514 nm laser source. Thermogravimetric analysis of the catalysts was carried out using a Setaram Labsys instrument enabling concurrent weight loss with its differential and heat flow changes (TG-DTA/DSC). The experiments were carried out in an N_2 atmosphere from 30 °C to 600 °C with a ramp rate of 5 °C/min. Ammonia temperature-programmed desorption analysis was carried out using a TPDRO 1100 series instrument (Thermo Electron Corporation). All of the samples were pre-treated in helium (1 h, 100 °C) followed by ammonia treatment (1 mL/min) and then ammonia desorption up to 700 °C in a flow of helium.

2.4. Glycerol dehydration

Evaluation of catalyst performance was carried out using a laboratory-scale microreactor (Fig. S1). The catalyst test equipment comprised of four main parts: syringe pump, pre-heater, catalytic reactor and cold traps for product collection. In addition, some experiments to probe longer-term catalyst performance were carried out using an HPLC pump in place of the syringe pump. The aqueous glycerol feed, 0.5–20 wt.%, was fed into the pre-heater (200 °C) at a liquid feed rate of 1 mL/h. The vapourised feed was then swept through the system and through the catalyst bed in a flow of inert nitrogen carrier gas (100 mL/min). All of the catalysts were pressed and sieved to a uniform particle size distribution of 250–425 μm before use and were packed into the 0.8 mm i.d. stainless steel reactor between plugs of silica wool. The catalysts (density of *ca.* 1 g/mL) were packed to a volume of 0.25–3 cm^3; the GHSV of the inert carrier was therefore 2000–24,000 h^{-1}. After exiting the reactor, the reaction products were collected in a series of cold traps. Three traps were used as this was found to be the most efficient method and ensured that any carry-over from the first trap was collected in subsequent traps. The contents of the cold traps were combined for analysis, which was performed offline using a Varian CP 3800 gas chromatograph equipped with capillary column (ZBWAX *plus*: i.d. 0.53 × 30 m). Gas samples were also collected and analysed offline by means of a Varian CP 3800 GC with a Porapack Q: 1/8″ × 2 m column. Mass balances were calculated to be 99% +5% for all reactions.

3. Results and discussion

Initially, catalysts were investigated using a low concentration of glycerol (0.5 wt.%) to evaluate the effect of the various preparation techniques on acrolein selectivity. Different loadings of silicotungstic acid on Al_2O_3-1 catalysts were tested at 315 °C for 3-h time-on-stream (Table 1). The alpha-alumina-supported catalysts have been reported previously as being suitable materials for the preparation of acrolein [17]. As described previously, acid-catalysed double dehydration of glycerol **a** leads predominantly to acrolein **b** (Fig. 1). Inevitably, however, especially given that hot acidic conditions are necessary to effect this transformation, by-products are formed. Those identified in the present studies are hydroxyacetone, ethanal, propanal, allyl alcohol, propene and acetone; these were measured using gas chromatography and identified by comparison with authentic samples. While purely speculative, it is possible to deduce reasonable mechanisms to explain the formation of the two major by-products, hydroxyacetone **d** and ethanal **h**. The former compound is most likely formed by an initial dehydration involving a primary hydroxy group of glycerol. This would produce the enol **c**, tautomerisation of which would then lead to the observed product **d** (Fig. 2).

A likely pathway to ethanal **h** features a *retro*-aldol reaction as shown in Fig. 3. In this case, an initial dehydration of the secondary hydroxy group in glycerol would lead to the isomeric enol **e**, tautomerisation of which would then give the hydroxy-aldehyde **f**, 3-hydroxypropanal, which is well set up, especially under acidic conditions, to undergo fragmentation, as shown in Fig. 3. Although ethanal **h** was detected, formaldehyde **g**, or obvious products arising from formaldehyde, such as formic acid, was not. However, decomposition is also likely or simply loss of this highly volatile product may explain why it was not detected. Perhaps significantly, only a trace quantity of carbon dioxide was detected amongst the various products.

Table 1
Product selectivities (in mol.%) obtained from glycerol (0.5 wt.%) dehydration over various catalysts at 315 °C, GHSV 24,000 h^{-1}, 3 h reaction duration.

Catalyst	Product selectivities (mol%)					
	Acrolein	Acetol	Ethanol	Propanal	Acetone	Allyl alcohol
0STA-1	21	21	11	1	44	3
20STA-1	74	4	13	1	8	0
30STA-1	80	2	12	2	7	0
40STA-1	80	1	12	1	6	0
50STA-1	78	–	14	1	6	0

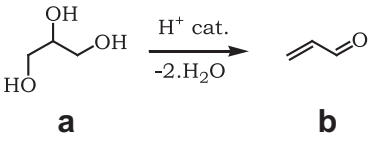

Fig. 1. Acrolein **b** formation from glycerol **a**.

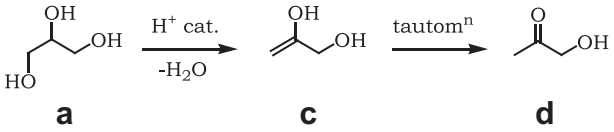

Fig. 2. Hydroxyacetone **d** formation.

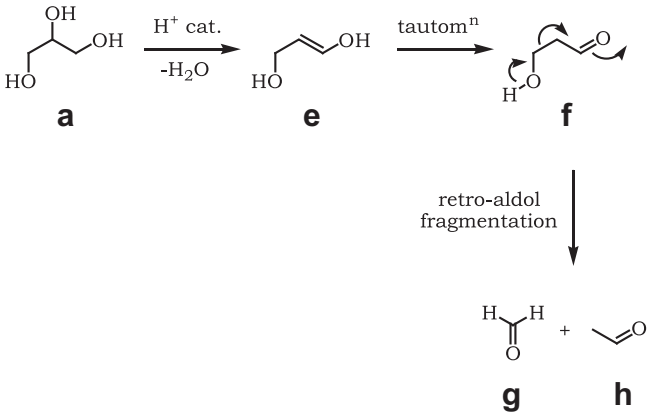

Fig. 3. Ethanal **h** formation.

The origins of the remaining and less abundant by-products are not so clear. One obvious pattern is that all of these compounds, propanal, allyl alcohol, propene and acetone, can be viewed as deriving from the reduction of other products. Thus, propanal could be formed by hydrogenation of acrolein **b**, allyl alcohol from C═O reduction of the same major product, propene from hydrogenolysis of allyl alcohol; a similar reaction would give acetone from hydroxyacetone **d**. Of course, other hydrogenolyses of C—O bonds in earlier precursors or even in glycerol itself could also lead to these by-products. One feature in favour of this deduction is that additional experiments in this area using related catalysts have clearly shown that a reducing atmosphere is generated during such dehydrations, for reasons that are not entirely clear at present.

The supported 30% silicotungstic acid catalyst (30STA-1), the best performing catalyst from the initial investigations, was tested at different temperatures to determine the effect on acrolein selectivity and glycerol conversion (Table 2). As the glycerol feed concentration was relatively low, relatively low reaction temperatures were possible compared to 300–400 °C, which are typically required [15,17]. Consequently, complete conversion

Table 2
Product selectivities (in mol.%) obtained from glycerol (0.5 wt.%) dehydration over 30STA-1 catalyst over different reaction temperatures. GHSV 24,000 h^{-1}, 3-h reaction duration. All at 100% glycerol conversion.

Temperature (°C)	Acrolein	Acetol	Ethanal	Acetone	Propanal	Acrylic acid	STY[a]
175	85	7	4	1	1	–	3.03
200	86	10	–	–	–	–	3.04
230	91	8	–	–	–	2	3.3
250	92	6	–	–	–	2	3.31
290	86	3	5	4	1	–	3.04
315	79	2	12	7	2	–	2.82
400	35	–	55	6	3	–	1.39

[a] Space time yield ($g_{(acrolein)}$ $kg^{-1}_{(cat)}$ h^{-1}).

was possible at lower temperatures. However, it was found that the maximum acrolein selectivity was favoured over a temperature range of 200–290 °C (Table 2). We consider that the acrolein selectivity decreased above this temperature range due to the preferential formation of ethanal via the retro-aldol fragmentation pathway illustrated in Fig. 3. This could be due to a change in the acidity of the active sites or a loss of the supported Keggin structure. For the reaction carried out at 250 °C, the acrolein selectivity was high at 92% and at 100% glycerol conversion, and it was sustained for 3-h time-on-stream.

Further testing of the 30STA-1 catalyst was conducted by increasing the glycerol feed concentration to 20 wt.%. Increasing the glycerol feed concentration affected the catalyst stability, resulting in a decrease of activity, particularly at lower temperatures (270–300 °C) (Fig. 4). Condensation of glycerol (b.p. 290 °C) on the catalyst surface at these temperatures is considered as the cause of the rapid loss of conversion. Therefore, reactions were performed at higher temperatures, and the effect on acrolein selectivity was observed. Reactions carried out at 270 °C to 330 °C resulted in an acrolein selectivity of *ca.* 90%. However, the acrolein selectivity decreased to *ca.* 85% following an increase in the reaction temperature to 360 °C. The investigation of reaction temperature was carried out over 4-h time-on-stream. The temperature at which the acrolein yield was found to be highest and the glycerol conversion sustained (330 °C) was applied to a longer reaction time (24 h). Product analysis over 24 h online revealed that an acrolein selectivity of *ca.* 90% was maintained for the first 7-h on-stream and 100% glycerol conversion was maintained. However, beyond 7 h, the selectivity decreased to around 80% with conversion decreasing to *ca.* 30% (Fig. 4). Carbonaceous deposits and the loss of activity are common with acidic catalysts used for glycerol dehydration [16,22]. Co-fed oxygen is one technique to reduce coking; however, this is associated with an increase in carbon oxide formation [24].

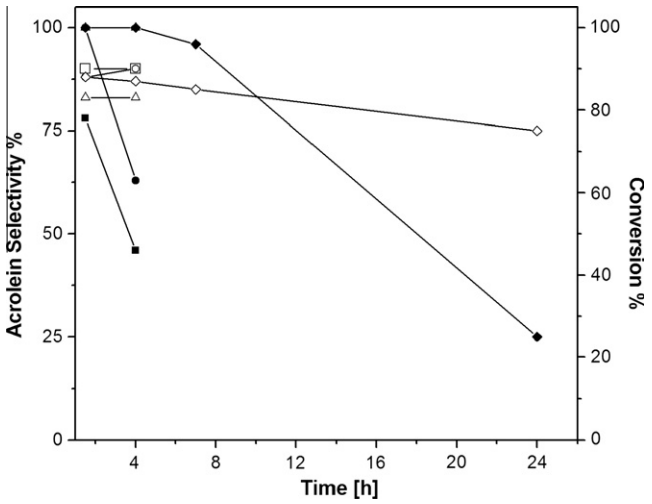

Fig. 4. Time-on-stream glycerol conversion (closed symbols) and acrolein selectivity (open symbols) over 30STA-1 catalyst at different temperatures. Conditions 20 wt.% glycerol feed, 1.2 mL/h, GHSV 2000 h^{-1}. *T*; ■/□ = 270 °C, ●/○ = 300 °C, ♦/◇ = 330 °C and ▲/△ = 360 °C.

In an effort to improve catalyst selectivity and stability for reactions without co-fed oxygen, a range of catalyst formulations were again tested with a lower glycerol concentration. From this secondary screening, rubidium- and caesium-doped silicotungstic acid catalysts were found to achieve high selectivity to acrolein at high glycerol conversion (Table 3). Over the lowest concentration of caesium and rubidium, i.e. 0.05 M-doped STA catalysts, a selectivity of 96% and 94%, respectively, at 100% glycerol conversion was obtained. However, silicomolybidic and phosphomolybidic acid doped with caesium were not as selective or as active in comparison. This loss of catalytic activity may be due to loss of structure of the molybdenum compounds and complete decomposition of the acid to metal oxide at the reaction temperature studied [19].

The best performing catalysts from this secondary screening (Cs0.05/STA and Rb0.05/STA) were then selected to be supported on Al_2O_3-1 and Al_2O_3-2 (XRD patterns shown in Fig. S2) and investigated with a higher glycerol feed concentration (10 wt.%) (Table 4). Initially, catalysts Cs/STA-1 and Rb/STA-1 both achieved a high acrolein selectivity of 91% at 100% conversion; however, the conversion decreased to *ca.* 37% and 44%, respectively, after 10-h reaction time.

Metal-modified STA catalysts were supported on Al_2O_3-2 analogously to those prepared with the Al_2O_3-1 support, and the effect on glycerol dehydration was studied (Table 5). With the Al_2O_3-2-supported catalysts, the maximum selectivity achieved was *ca.* 90% at 100% conversion in the case of the Cs/STA-2 catalyst at a temperature of 300 °C. In order to assess the catalyst stability further much longer time-on-stream studies were performed. The catalyst was found to be stable up to 90 h of reaction time with a 10 wt.% glycerol feed (Fig. 5). Conversion then decreased to *ca.* 75% beyond 90-h time-on-stream, decreasing further to *ca.* 55% after 198-h on-stream. The catalyst was able to be partially regenerated at 350 °C by flowing 5% oxygen (bal. nitrogen) for 24 h, regaining 90% conversion and 80% acrolein selectivity for a further 24-h on-stream at reaction temperature (Fig. 5). Furthermore, this catalyst was also tested at a higher feed concentration (20 wt.%), and the reaction was carried out for 10 h (Table 6). The catalyst was stable, maintaining glycerol conversion and acrolein selectivity; 100% and *ca.* 90%, respectively, resulting in a space time yield (STY) of 210 $g_{acrolein}$ kg^{-1}_{cat} h^{-1}. The space time yield achieved over the Rb/STA-2 catalyst was determined to be 195 $g_{acrolein}$ kg^{-1}_{cat} h^{-1}, and this was maintained over the 10-h reaction period. The high selectivity achieved with the supported metal-doped STA catalysts is considered to be related to the acid strength of the active sites. We have observed that generally with STA-based catalysts, the initial acrolein selectivity is high. The stability of these active sites

Table 3
Product selectivities (in mol.%) obtained from glycerol (0.5 wt.%) dehydration over various catalysts at 250 °C, GHSV 24,000 h^{-1}, 3-h reaction duration.

Catalyst	Conversion (%)	Acrolein	Acetol	Ethanal	Propanal	Acetone	Acrylic acid	STY[a]
Cs0.05/STA	100	96	4	–	–	–	–	3.49
Cs0.15/STA	10	27	27	–	–	–	22	0.01
Cs0.25/STA	97	93	5	–	–	–	3	3.1
Cs0.35/STA	2	0	44	–	–	–	56	0
Cs0.25/SMA	31	26	5	24	2	6	7	0.08
Cs0.25/PMA	23	33	7	11	–	–	11	0.06
Rb0.05/STA	100	94	4	–	–	–	2	3.32
Rb0.15/STA	100	92	7	–	–	–	2	3.26
Rb0.25/STA	82	90	8	–	–	–	2	2.14

[a] Space time yield ($g_{(acrolein)}$ $kg^{-1}_{(cat)}$ h^{-1}).

Table 4
Product selectivities (in mol.%) obtained from glycerol (10 wt.%) dehydration over Al_2O_3-1-supported Cs- and Rb-doped STA catalysts. GHSV 12,000 h^{-1}.

Catalyst	Temperature (°C)	Time (h)	Conversion (%)	Acrolein	Acetol	Ethanal	Propanal	Acetone	STY[a]
Cs/STA-1	300	1.5	100	91	9	–	–	–	99
		5	66	87	10	1	1	–	41
		10	37	85	13	–	1	2	12.4
	330	1.5	100	89	6	2	2	1	95.5
		5	60	84	10	4	1	1	32
		10	31	83	11	4	1		8.7
Rb/STA-1	300	1.5	87	91	6	1	1	1	74
		5	54	88	10	1	1	1	28
		10	35	88	9	2	1	1	12
	330	1.5	100	91	4	3	1	1	100
		5	69	85	10	3	1	1	43.3
		10	44	84	12	3	1	1	17.7

[a] Space time yield ($g_{(acrolein)}$ $kg^{-1}_{(cat)}$ h^{-1}).

Table 5
Product selectivities (in mol.%) obtained from glycerol (10 wt.%) dehydration over Al_2O_3-2-supported STA and Cs- and Rb-doped STA catalysts. GHSV 12,000 h^{-1}.

Catalyst	Temperature (°C)	Time (h)	Conversion (%)	Acrolein	Acetol	Ethanal	Propanal	Acetone	STY[a]
30STA-2	300	1.5	83	75	6	8	6	1	41
		5	100	73	5	9	8	1	79
		10	100	71	8	9	7	2	77
Cs/STA-2	300	1.5	97	88	6	4	2	1	94
		5	100	87	9	3	1	–	98
		10	100	84	11	3	1	1	96
	330	1.5	100	78	4	13	3	2	89
		5	100	77	9	11	2	1	84
Rb/STA-2	300	1.5	100	83	4	1	2	1	91
		5	100	79	8	4	2	1	87
	330	1.5	100	75	4	15	3	1	85
		5	100	73	8	10	2	1	83

[a] Space time yield ($g_{(acrolein)}$ $kg^{-1}_{(cat)}$ h^{-1}).

based on the Keggin structure has been improved by partially doping the STA with Cs or Rb and supporting on Al_2O_3-2. Therefore, the catalyst acidity is maintained at the desired strength, typically thought of over a HA range of −2 to −8 [10,13,14], and this is crucial for high acrolein selectivity [15,16]. We will discuss the stability of the active site with respect to the high acrolein yield further with the aid of various characterisation techniques.

The stability of the alumina-supported catalysts over reaction times of 10 h was investigated. Al_2O_3-1-supported catalysts were found to be less stable for time-on-stream studies when compared to theta-delta Al_2O_3-2-supported catalysts. Alpha-alumina is thought to be the most stable phase of alumina, which is related to its low surface area obtained upon heating boehmite (AlOOH). In this phase, Al^{3+} cations occupy only 2/3 of the octahedral interstitial sites corresponding to its low surface area when compared to theta-delta Al_2O_3-2. This phase contains a monoclinic spinel superstructure, in which Al^{3+} ions occupy more than 13 out of 16 octahedral sites for delta and they are distributed equally amongst octahedral and tetrahedral sites for the theta phase, which have up to 480 vibrational modes, making it highly surface active [25–28]. The catalysts with this stable, low surface area Al_2O_3-1 support (Table S1) resulted in very weak interactions with the deposited acid species [13]. For long-term catalytic activity of silicotungstic acid-based catalysts, a strong interaction of the silicotungstic acid with the support is desirable [29]. This strong interaction provides stability under the high temperature conditions required for glycerol dehydration [17]. Thermal analysis of the Al_2O_3-1-supported catalysts illustrates the instability associated with this weaker interaction. The lower stability can be related to the presence of an exothermic peak at around 500 °C in the heat flow analysis profile (Fig. 6). This feature is related to undispersed or weakly bound silicotungstate species on the support [15,17]. These species are considered to decompose during the glycerol dehydration reaction resulting in a loss of catalytic activity. However, this thermal

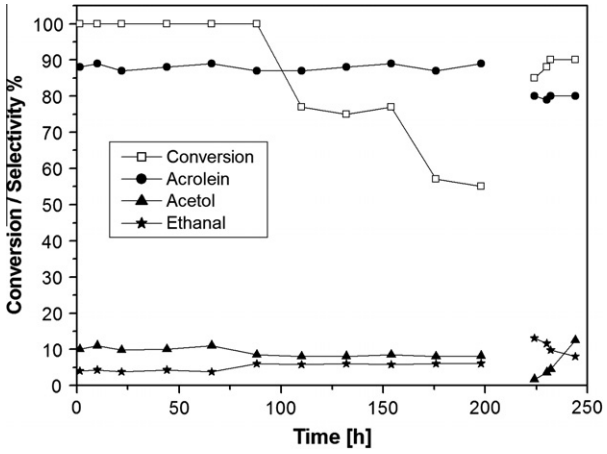

Fig. 5. Time-on-stream glycerol conversion and acrolein selectivity over Cs/STA-2 catalyst at 300 °C with a period of regeneration. Conditions 10 wt.% glycerol feed, 1 mL/h, GHSV 6000 h^{-1}. Catalyst regeneration at 200 h, 350 °C for 24 h with 5% O_2 in N_2 (100 mL/min).

Table 6
Product selectivities (in mol.%) obtained from glycerol (20 wt.%) dehydration over various catalysts at 300 °C, GHSV 6000 h^{-1}, 10-h reaction duration.

Catalyst	Conversion (%)	Acrolein	Acetol	Ethanal	Propanal	Acetone	STY[a]
Cs/STA-2	100	88	8	2	1	1	210

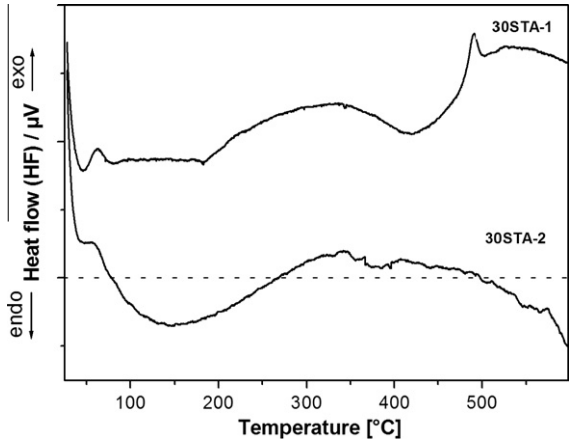

Fig. 6. Heat flow analysis of 30STA catalysts supported on alumina (1 and 2), dotted line: zero heat flux.

transition was not present with the Al_2O_3-2-supported catalysts, which showed stronger binding of the silicotungstic acid with the support, resulting in increased catalyst stability (Fig. 6).

In the case of caesium-doped silicotungstic acid catalysts, where an increase in the Cs concentration led to a decrease in activity, a similar trend prevails. Cs (0.05 M)-doped silicotungstic acid partially replaces the $H_5O_2^+$ moiety of silicotungstic acid which can be seen in the form of an exothermic peak around 500–550 °C and is attributed to instability of the modified silicotungstic acid species. However, at loadings above 0.05 M, the $H_5O_2^+$ moiety of silicotungstic acid was completely replaced with Cs^+ to form a stable Cs-doped silicotungstate phase [30,31]. Therefore, at higher loadings, no exothermic response was observed in the heat flow analysis profile (Fig. 7). The heat flow features recorded at 100 and

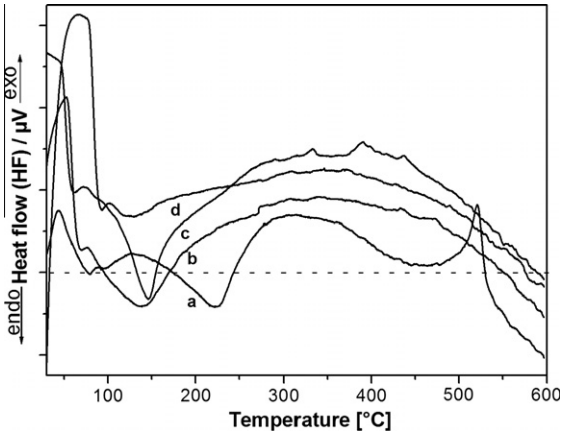

Fig. 7. Heat flow analysis of Cs-doped STA catalysts; *a* = Cs0.05/STA, *b* = Cs0.15/STA, *c* = Cs0.25/STA and *d* = Cs0.35/STA, dotted line: zero heat flux.

200 °C are considered to be due to the removal of physisorbed and hydrated water from the heteropoly acid [30]. Those features found in the range of 200 °C and 300 °C are considered to be due to structural changes of the partially doped acid species which are not visible with other fully doped STA catalysts [32]. The same behaviour was observed with rubidium-doped silicotungstic acid catalysts (Fig. S3). Therefore, over the reaction temperatures used the structure of the metal-doped catalysts should be stable. However, supporting the fully doped STA material on the alumina leads to weak binding with the support due to the lack of available $H_5O_2^+$ which interacts with surface species on the support. In the case of the partially doped Cs/STA, supporting this material leads to improved binding due to the presence of the remaining $H_5O_2^+$ moieties. These enable the stronger STA–support interaction. Characterisation of the supported catalyst was conducted, and thermal analysis indicated that the caesium silicotungstate moiety supported on Al_2O_3-1 was weakly bound with an exothermic peak around 500 °C (Fig. 8a), and as mentioned previously, this is related to the STA decomposition. In the case of the catalysts supported on Al_2O_3-2, there was strong binding between the support and the caesium-doped silicotungstate species showing no exothermic response for unbound or weakly bound species (Fig. 8b). In addition, the partially doped Cs/STA materials on both supports (Al_2O_3-1 and 2) no longer have endothermic heat transitions associated with the instability of the Keggin structure. For the supported Rb/STA materials, a similar trend emerges with respect to the Keggin struc-

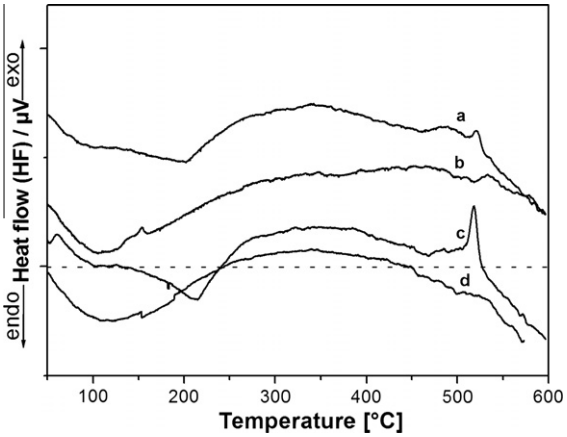

Fig. 8. Heat flow analysis of Cs- and Rb-doped STA catalysts supported on alumina (1 and 2); *a* = Cs/STA-1, *b* = Rb/STA-2, *c* = Rb/STA-1, *d* = Cs/STA-2, dotted line: zero heat flux.

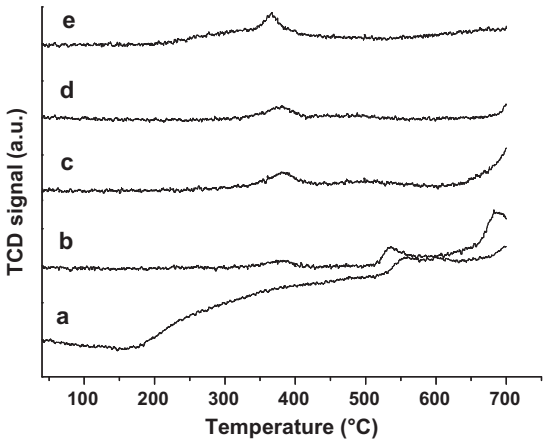

Fig. 9. Ammonia thermal-programmed desorption analysis of Cs-doped STA catalysts, *a* = Cs0.05/STA (with no NH3 pre-treatment), *b* = Cs0.05/STA, *c* = Cs0.15/STA, *d* = Cs0.25/STA and *e* = Cs0.35/STA.

ture, instability due to a transition at *ca.* 200 °C for the Rb/STA-1. The transition at 500 °C is related to weak binding to the support which is not present for the Rb/STA-2 (Fig. 8c and d).

The nature of acidic sites, i.e. weak, medium or strong, on the catalyst surface was determined by ammonia temperature-programmed desorption. The classification of acid site strength is considered as follows: weak (150–300 °C), medium (300–500 °C) and strong (⩾500 °C) [33]. Catalysts doped with different concentrations of caesium were analysed (Fig. 9). All materials possess acid sites of medium strength. However, we observe decomposition of the STA structure at higher temperatures. This is confirmed by the TPD analysis the Cs0.05/STA sample which was not pre-treated with NH_3, which showed significant desorption of decomposition products at *ca.* 550 and 700 °C (Fig. 9a). The slow rise of the TCD response over the temperature range is considered to be due to thermal expansion of the carrier gas. The best performing catalyst (Fig. 9b) has a low density of medium acid sites, whereas the catalyst with the highest density of medium sites and a broader feature present in the TPD profile has the highest Cs loading and exhibits poor catalytic activity.

Considering the differences in the catalysts prepared on different alumina supports, ammonia TPD indicated that the Al_2O_3-2 support contained a broad range of acidic sites (weak, medium and strong), and they were in greater density when compared to the Al_2O_3-1 support, which contained only small amounts of medium acid sites (Fig. 10). Analysis of the CsSTA-2 catalyst without NH_3 pre-treatment indicated that the material was stable over the temperature range investigated.

Laser Raman spectroscopy was used for the analysis of Keggin structure for the unsupported Cs-doped STA catalysts in Fig. S4. The transitions shown at *ca.* 998 cm^{-1} are attributed to the W=O stretch, *ca.* 974 cm^{-1} for W—O—W bending, *ca.* 850 for W—O—W stretching, *ca.* 555 cm^{-1} for O—Si—O bending, while those at 110, 150 and 225 cm^{-1} are associated with WO_3 [34]. There is a loss of several transitions related to the Keggin structure with the highest Cs loading, and we attribute this to the distortion of the STA structure. Caesium addition induces a contraction effect on the STA structure as Cs replaces the $H_2O_5^+$ moieties [35]. This corresponds to the X-ray analysis results in which the reflection related to the Cs/STA phase found at 26° is completely lost in the case of 0.35 M catalyst (Fig. S5). As previously reported, silicotungstic acid needs strong binding sites on the supporting material in order to maintain the active silicotungstate phase over a long time period at a higher temperature [17]. Intense stretching and bending vibrational bands of tungsten-oxygen were seen in the Raman shift for the weakly bound caesium silicotungstate species on Al_2O_3-1 (Fig. 11c), as compared to the weak band found with Al_2O_3-2 (Fig. 11a). Moreover, in the case of Cs/STA-2, the main W=O stretching, and the W—O—W bending shoulder band, was less defined and along with the shifting of the W—O—W stretch towards lower wavelength, which is considered to be due to the bond weakening/distortion by strong interaction with the surface of the alumina-2 support [15,36]. Analysis of the υ(W=O) transition after use indicates that the stability of the silicotungstate is lower with the weakly bound species on Al_2O_3-1 (Fig. 11d) when compared to the species on Al_2O_3-2 which retains this transition (Fig. 11b).

XRD patterns for the bulk silicotungstic acid show distinct reflections from (220), (310), (222), (400), (411), (420), (332) and (510) lattice planes reported by Pizzio et al. [30], which can be seen in the lower concentration caesium catalyst along with the new crystalline peaks of caesium-doped silicotungstate species (Fig. S5) [31]. However, in the case of fully doped silicotungstic acid catalysts, the parent STA phases are replaced with the Cs/STA phases showing complete doping. The caesium- and rubidium-doped silicotungstic acid catalysts were found to be selective for acrolein over 3-h on-stream, however, at a low

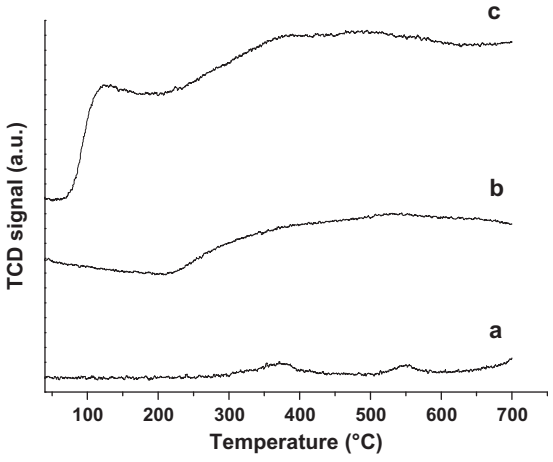

Fig. 10. Ammonia thermal-programmed desorption analysis of Cs-doped STA supported on alumina (1 = *a* and 2 = *c*) catalysts, *b* = Cs/STA-2 with no NH3 pre-treatment.

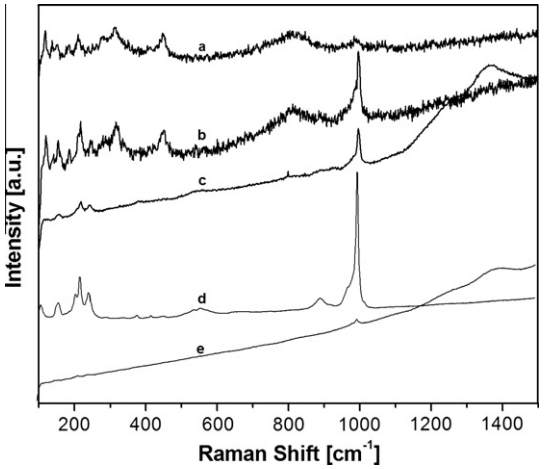

Fig. 11. Raman spectroscopy of Cs-doped STA catalysts supported on alumina prior to reaction and postreaction. *a* = Rb/STA-2; fresh, *b* = Cs/STA-2; fresh, *c* = Cs/STA-2; used and *d* = Cs/STA-1; fresh and *e* = Cs/STA-1; used.

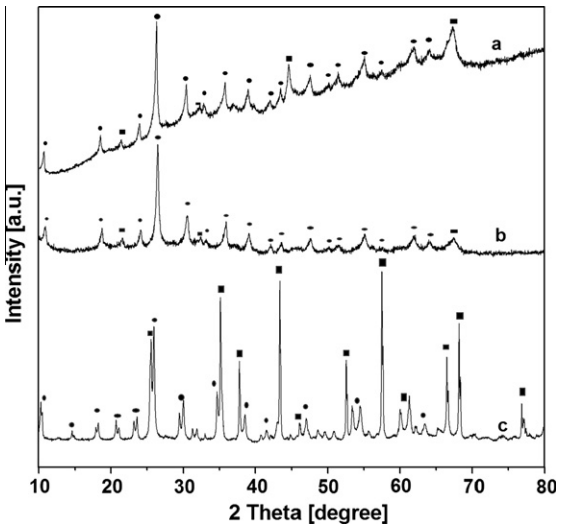

Fig. 12. X-ray diffraction patterns of Cs-doped supported STA (1 and 2), *a* = Cs/STA-2 fresh, *b* = Cs/STA-2 used (10 h reaction), *c* = Cs/STA-1 fresh, (circles = Cs/STA species and blocks = respective Al_2O_3 support).

glycerol feed concentration. These catalysts are reported to have insufficient stability over a longer reaction time to tolerate higher glycerol feed concentrations [17,20]. Thermal analysis of the most selective catalyst, the partially doped Cs/STA, indicated that it would not be sufficiently stable over a longer reaction time with higher feed concentrations. Therefore, for use under increased glycerol feed conditions, the stability and long-term activity of the Cs-based STA would require a support.

Partially caesium- and rubidium-doped STA catalysts were supported on alumina, and the delta-theta-Al_2O_3-supported catalysts were stable for longer reaction times compared to the alpha-Al_2O_3 catalysts. The XRD pattern for Al_2O_3-1 support has the characteristic diffraction reflections of the alpha phase (Fig. S2) (ICDD ref. code 01-078-2427). These diffraction reflections further indicate that the binding of the doped STA is weak as we observed additional peaks in the case of catalyst (for caesium-doped silicotungstic acid phase) (Fig. 12) [31]. However, in the case of Al_2O_3-2 support, there is strong interaction between the support and the active material as distinct reflections for the Al_2O_3-2 support were not observable (Fig. 12). The diffraction pattern for the Cs/STA-2, which had undergone catalyst testing for 10 h, indicated that there was no observable loss of the Cs/STA species (Fig. 12b).

4. Conclusions

Acidic heteropoly anion-based catalysts have been prepared and evaluated for the catalytic dehydration of glycerol. Initially, catalysts were screened at various temperatures and with different glycerol feed concentrations. Rubidium- and caesium-doped silicotungstic acid catalysts were found to be very selective for acrolein formation. However, these unsupported catalysts were not stable over longer reaction times even with a low glycerol feed concentration (0.5 wt.%). Supporting these partially doped catalysts on Al_2O_3-1 (alpha) did not result in a stable catalyst. However, supporting caesium-doped silicotungstic acid on Al_2O_3-2 (mixture of theta and delta phases) was found to be stable for up to 90-h reaction time and gave a maximum selectivity of *ca.* 90% acrolein along at 100% glycerol conversion with a space time yield of 105 $g_{acrolein}\ kg_{cat}^{-1}\ h^{-1}$ (10 wt.% glycerol). When the glycerol feed concentration was increased to 20 wt.% glycerol, a space time yield of 210 $g_{acrolein}\ kg_{cat}^{-1}\ h^{-1}$ was achieved, although it was stable for a shorter time-on-stream. This catalyst appears, to the best of our knowledge, to be the most stable silicotungstic acid-derived catalyst and one that does not require oxygen in the feed gas to achieve stable operation. Analysis of the catalysts suggests that the origin of the long-term stability is related to the strength of the partially doped silicotungstic acid on the alumina support. Doping with caesium maintains the Keggin structure of the silicotungstic acid, resulting in long-term stability and high acrolein yield observed.

Acknowledgments

This work formed part of the Glycerol Challenge. The Technology Strategy Board is thanked for their financial support. This project is co-funded by the Technology Strategy Board's Collaborative Research and Development programme, following an open competition. The Technology Strategy Board is an executive body established by the Government to drive innovation. We thank Vertellus Specialities Chemicals, USA, for the alumina supports used in this study.

Appendix A. Supplementary material

Supplementary data associated with this article can be found, in the online version, at doi:10.1016/j.jcat.2011.11.004.

References

[1] A.J. Ragauskas, C.K. Williams, B.H. Davison, G. Britovsek, J. Cairney, C.A. Eckert, W.J. Frederick Jr., J.P. Hallett, D.J. Leak, C.L. Liotta, J.R. Mielenz, R. Murphy, R. Templer, T. Tschaplinski, Science (Washington, DC, US) 311 (2006) 484–489.
[2] M. Snare, I. Kubickova, P. Maeki-Arvela, D. Chichova, K. Eraenen, D.Y. Murzin, Fuel 87 (2008) 933–945.
[3] United Nations Framework Convention on Climate Change. <http://unfccc.int>.
[4] B. Katryniok, S. Paul, V. Belliere-Baca, P. Rey, F. Dumeignil, Green Chem. 12 (2010) 2079–2098.
[5] G.W. Keulks, L.D. Krenzke, T.M. Notermann, Adv. Catal. 27 (1978) 183–225.
[6] L.D. Krenzke, G.W. Keulks, A.V. Sklyarov, A.A. Firsova, M.Y. Kutirev, L.Y. Margolis, O.V. Krylov, J. Catal. 52 (1978) 418–424.
[7] J. Hagen, Industrial Catalysis: A Practical Approach (1999) 440.
[8] B. Katryniok, S. Paul, M. Capron, F. Dumeignil, ChemSusChem 2 (2009) 719–730.
[9] L.P. Hammett, A.J. Deyrup, J. Am. Chem. Soc. 54 (1932) 4239–4247.
[10] A. Neher, T. Haas, D. Arntz, H. Klenk, W. Girke, US Patent 5387720, 1995.
[11] S. Kuba, P. Concepcion Heydorn, R.K. Grasselli, B.C. Gates, M. Che, H. Knozinger, Phys. Chem. Chem. Phys. 3 (2001) 146–154.
[12] B. Katryniok, S. Paul, M. Capron, C. Lancelot, V. Belliere-Baca, P. Rey, F. Dumeignil, Green Chem. 12 (2010) 1922–1925.
[13] S.-H. Chai, H.-P. Wang, Y. Liang, B.-Q. Xu, Green Chem. 9 (2007) 1130–1136.
[14] S.-H. Chai, H.-P. Wang, Y. Liang, B.-Q. Xu, J. Catal. 250 (2007) 342–349.
[15] S.-H. Chai, H.-P. Wang, Y. Liang, B.-Q. Xu, Appl. Catal. A 353 (2009) 213–222.
[16] E. Tsukuda, S. Sato, R. Takahashi, T. Sodesawa, Catal. Commun. 8 (2007) 1349–1353.
[17] S.-H. Chai, H.-P. Wang, Y. Liang, B.-Q. Xu, Green Chem. 10 (2008) 1087–1093.
[18] H. Atia, U. Armbruster, A. Martin, J. Catal. 258 (2008) 71–82.
[19] S. Erfle, U. Armbruster, U. Bentrup, A. Martin, A. Brueckner, Appl. Catal. A 391 (2011) 102–109.
[20] A. Alhanash, E.F. Kozhevnikova, I.V. Kozhevnikov, Appl. Catal. A 378 (2010) 11–18.
[21] H. Atia, U. Armbruster, A. Martin, Appl. Catal. A 393 (2011) 331–339.
[22] J.L. Dubois, C. Duquenne, W. Holderich, FR Patent 2005-1499-2882052, 2006.
[23] Y. Magatani, K. Okumura, J.-L. Dubois, J.-F. Devaux, WO Patent 2009-JP67115-2011033689, 2011.
[24] F. Wang, J.-L. Dubois, W. Ueda, Appl. Catal. A 376 (2010) 25–32.
[25] A. Boumaza, L. Favaro, J. Ledion, G. Sattonnay, J.B. Brubach, P. Berthet, A.M. Huntz, P. Roy, R. Tetot, J. Solid State Chem. 182 (2009) 1171–1176.
[26] P. Colomban, J. Mater. Sci. 24 (1989) 3002–3010.
[27] N. Fremy, V. Maurice, P. Marcus, Surf. Interface Anal. 34 (2002) 519–523.
[28] G. Paglia, A.L. Rohl, C.E. Buckley, J.D. Gale, Phys. Rev. B: Condens. Matter Mater. Phys. 71 (2005) 224115.
[29] I.V. Kozhevnikov, Chem. Rev. (Washington, DC) 98 (1998) 171–198.
[30] L.R. Pizzio, M.N. Blanco, Micropor. Mesopor. Mater. 103 (2007) 40–47.
[31] J.A. Santos, Proc. Roy. Soc. London, Ser. A 150 (1935) 309–322.
[32] A.A. Babad-Zakhryapin, Izv. Akad. Nauk SSSR, Ser. Khim. (1963) 215–220.
[33] J.C. Yori, J.M. Grau, V.M. Benitez, J. Sepulveda, Appl. Catal. A 286 (2005) 71–78.
[34] P. Sabatier, G. Gaudion, Comptut. Rend. 166 (1918) 1033–1039.
[35] L. Pesaresi, D.R. Brown, A.F. Lee, J.M. Montero, H. Williams, K. Wilson, Appl. Catal. A 360 (2009) 50–58.
[36] R. Thouvenot, M. Fournier, R. Franck, C. Rocchiccioli-Deltcheff, Inorg. Chem. 23 (1984) 598–605.